Printed in Geophys. J. Int. (2000) **141,** 241–252. This edited version differs from the printed one because of some minor language change and of course of the pagination. The content is the same. Email barba@ingv.it, or basili_r@ingv.it.
Citation: Barba S. and Basili R.. Analisys of seismological and geological observations for moderate-size earthquakes: the Colfiorito Fault System (Central Apennines, Italy), Geophys. J. Int. (2000) **141**, 241-252.

Analysis of seismological and geological observations for moderate-size earthquakes: the Colfiorito Fault System (Central Apennines, Italy)

Salvatore Barba & Roberto Basili

Abstract

To contribute to the understanding of the relationships between moderate earthquakes and the faults that are recognisable in the geological record, we analysed seismological and geological data related to the 1997-98 Umbria-Marche (Central Italy) earthquake swarm. **The seismological recordings, collected by local networks, allowed accurate location of about 1000 events, whereas the geological field-observations provided a picture of the structural features and the ground-surface deformations. We also re-examined and utilised some already published data and results, mostly about the fault plane solutions and the geology.**

On the basis of earthquake locations, fault plane solutions, and geological mapping we explored the possible correlation between the earthquake causative fault-planes and the normal faults exposed in the area. Our results show that the two mainshocks that occurred on September 26, 1997 (M_W=5.7 and M_W=6.0) originated on the same structure reactivating at depth the Colfiorito normal faults. Both ruptures did not propagate up to the ground surface but triggered gravitational sliding that occurred along pre-existing fault scarps. The earthquake that occurred on October 14, 1997 (M_W=5.6) originated on another fault-branch at a much shallower depth. In spite of the lower magnitude, this earthquake produced tectonic ruptures where the fault plane projects to the surface in an area where no faults were previously mapped.

By comparing the paleostress reconstruction, based on slickenside lineations analysis, and the focal mechanism solutions, we also suggest a possible correlation between the long-term (Early-Middle Pleistocene) cumulative effects of the Colfiorito Fault System and the short-term behaviour of the fault planes observed during this earthquake swarm, favouring the idea of a seismogenic source producing clustered moderate-size earthquakes rather than large events scattered in time.

~~Our results suggest that the integration of geological and seismological observations can constrain the seismotectonic interpretations in regions of low level seismicity and that this integration can pose a reliable basis in the seismic hazard assessment.~~

Keywords: Earthquake, Normal faulting, Seismotectonics, Central Apennine, Italy

Introduction

Empirical relationships between earthquake magnitude and rupture dimensions (Bonilla, Mark & Lienkaemper, 1984; Bonilla, 1988; Wells & Coppersmith, 1994) show that for magnitude M<6 the signature at the ground surface of coseismic ruptures is very faint. Such ruptures fall in the size range of many other surface deformation features that could be originated by ground shaking and therefore, it could be very difficult to detect them in the field and to correctly **identify the active faults**. In regions characterised by a moderate level of seismicity, the long-term cumulative effects of coseismic ruptures could give rise to unclear structural patterns, which, in turn, greatly hinder the understanding of the overall seismotectonic setting. Notwithstanding, M>5 multiple earthquakes are able to produce severe damages **and therefore they are of great societal interest.** ~~and, therefore, the above mentioned difficulties have compelling implications in seismic hazard assessment.~~

The **area where the 1997-98 Colfiorito earthquakes occurred** ~~seismic swarm that occurred in central Italy during the last autumn 1997 (~~(Umbria-Marche region, in the northern part of the Central Apennines, fig. 1) is a typical example of the problem described above. On one side, several moderate earthquakes struck this area in historical time (Boschi *et al.*, 1997), while instrumentally detected sequences occurred in 1979 near Norcia (mainshock M_S=5.8, Deschamps, Iannaccone & Scarpa, 1984), about 30 km south-east of Colfiorito, and in 1984 near Gubbio (mainshock M_S=5.3, Haessler at al., 1988), about 45 km to the north-west. On the other side, many Quaternary **normal** faults ~~and some active normal faults that have been reviewed in literature~~ characterise the tectonic setting of the region (from North to South: Menichetti, 1992, for the Gubbio area; Bosi, Coltorti & Dramis, 1983, unpublished map of the Gualdo Tadino zone; Calamita & Pizzi, 1992, and Cello *et al.*, 1997, for the southern zone). Such faults are generally up to 15 km long, strike NW-SE, plunge to SW, and have mainly dip-slip kinematics. **Cello *et al.* (1997) report also** N-S trending **left-lateral** strike-slip faults. **In addition, GPS-based methods have not yet allowed isolating extension loci, probably because of the low extension rate and the mainly vertical tectonics. In fact, the relationship between outcropping and seismogenic faults is not yet clear.**

The seismic swarm analysed in this work began on September 3, 1997 and during the subsequent two months, it was characterised by more than 25 earthquakes with M>4.0.

On September 26, 1997 two earthquakes occurred near the Colfiorito village, the first at 00:33 GMT (M_W=5.7) and the second at 09:40 GMT (M_W=6.0), causing severe damages, a few casualties and many injuries. Socio-economic life of this historical district was literally shaken, and its major symbol, the Basilica of San Francesco in Assisi, was severely damaged. On October 14 at 15:23 GMT another M_W=5.6 earthquake occurred about 15 km to the South, near the village of Sellano. Then, during the subsequent few months the seismic activity continued to the Northwest, extending the fractured area by more than 50 km.

Starting just after the first mainshock, several field surveys have been carried out in the epicentral area by different research institutions; seismological data were collected by temporary weak and strong motion networks managed by Istituto Nazionale di Geofisica (ING) and Servizio Sismico Nazionale (SSN), deployed to improve permanent stations coverage (Barba, Di Giovambattista & Smriglio, 1995; Berardi *et al.*, 1998). Geological investigations along with geodetic measurements were conducted by Istituto Geografico Militare, Gruppo Nazionale per la Difesa dai Terremoti (GNDT), ING, and Agenzia Nazionale Protezione Ambiente in order to collect data about geological effects and surface deformation features. A macroseismic survey, mainly conducted by SSN, provided instead a detailed picture of damage distribution (see Camassi *et al.*, 1997).

These surveys provided all the necessary data for a thorough description of the Colfiorito Fault System (CFFS) by different points of view. The most part of the seismicity is dealt with in Amato *et al.* (1998) and Cattaneo *et al.* (1998a, b) while source properties and kinematics are analysed by Zollo *et al.* (1998, 1999), Pino, Mazza & Boschi (1999), Ekström *et al.* (1998), and Olivieri & Ekström (1999). The analysis of geological features are treated in Basili *et al.* (1998), Cinti *et al.* (1999), Cello *et al.* (1998), and Meghraoui, Bosi & Camelbeek (1999). The results of geodetic observations, such as SAR interferometry, GPS data analysis and topographic levelling, are discussed by Stramondo *et al.* (1999), Hunstad *et al.* (1998), Basili & Meghraoui (1999), and De Martini, Marchioni & Valensise (1999), refining the picture of coseismic surface deformations.

Despite the large number of studies, many of which are still in progress, the relationships among (i) the seismogenic faults and their behaviour, (ii) the earthquake signatures at the surface, and (iii) the correlative structures recorded over geological time, are not yet clear. **Because directivity of the source and distance from the fault greatly influence the probable ground motion, i.e. the seismic hazard, it is necessary that relationships among points (i)–(iii) be better understood. To this purpose, we will try also to address the controversy among Basili *et al.* (1998), Cinti *et al.* (1999), and Cello *et al.* (1998).** ~~More in-depth studies became thus necessary to improve our understanding of the seismotectonics of the CFFS that will eventually help assess the seismic hazard of this area.~~

This paper combines seismological and geological data in order to contribute to the understanding of the role played during the seismic swarm by the faults exposed in the area and belonging to the CFFS. To this purpose we both reinterpreted some already published data and analysed new ones. Results suggest how and how much the integration of geological and seismological measurements constrain the seismotectonic interpretations and pose a reliable basis for the assessment of seismic hazards.

Geological background

The northern Apennine is an East-verging fold-and-thrust mountain belt overridden and accreted on the subducting Adria plate. Compressional tectonics progressively migrated toward the East, all along the Tertiary (66 - 1.81 Ma) and the Quaternary (<1.81 Ma), affecting Mesozoic-Paleogene (>30 Ma) passive margin carbonate sequences and Chattian-Pleistocene (<30 Ma) fore-deep terrigenous sequences. In addition to compression at the thrust leading edge, the mountain belt also experienced coeval back-arc extension combined with regional crustal uplift (Doglioni, 1997).

The area affected by the 1997-98 series of earthquakes is an elevated region on the rear of a long-wavelength anticline (Calamita & Pizzi, 1992) located just to the West of the current transition between the regions of extensional and compressional stress regimes (fig. 1).

As lately shown by deep seismic-reflection profile (Pialli, Barchi & Menichetti, 1991; Barchi, Minelli & Pialli, 1997) extension in this region was driven along low-angle **(~20°–30°)** East-dipping master normal faults. A number of antithetic (West-dipping) high-angle **(~40°–60°)** dip-slip normal faults join the masters at depth within the first 10-15 km of the crust (Doglioni *et al.* 1997; Boncio *et al.*, 1997) thereby forming a series of intermontane basins which alternate with NW-SE trending ranges. These last steeper faults lay at the eastern boundaries between the intermontane basins (half-grabens) and the surrounding uplands and left a strong imprint on the geologic and geomorphic record by controlling drainage and continental sedimentary in-fill.

Two main continental basins are present in the area which are clearly controlled by the CFFS: the Cesi-Forcella basin to the South, and the Colfiorito basin to the North (fig. 2). The southern basin probably developed in a dominant interior drainage, which is now captured at the South-end by head-ward erosion of a N-S trending valley. Late erosion contributed in exposing an Early-Middle Pleistocene sedimentary basin-filling (Ficcarelli *et al.*, 1997) which unconformably rests on the carbonate bedrock. The in-fill consists mainly by lacustrine clay sequences interbedded with fluvial pebble/gravel lenses. This sequence is capped by a palustrine deposit containing a 424 ka old pyroclastic layer (Ficcarelli *et al.*, 1997) and, locally, by Late Pleistocene alluvial fans. The Colfiorito basin, to the North, also developed in a dominant interior drainage but the sedimentary filling is much

less exposed due to the absence of a deep-incising fluvial network. However some Middle Pleistocene alluvial terrace deposits (Coltorti & Dramis, 1988) are exposed in the peripheral area of the basin, while in the middle a few outcrops provide sight of lacustrine clay sequences interbedded with fluvial gravel lenses. Lake environment persisted during Holocene and the basin was artificially drained in historical time.

Structural analysis

The main exposed faults of the area are approximately 5-8 km long, strike between 120° and 170° North, plunge to W-SW and dip about 50°-60°. At the outcrop scale the faults are marked by several tens metres thick gouge and by a few metres high bedrock fault scarps. Taking into account the age of the sedimentary in-fill of the basins and according to most of the geological literature of the region these faults could be considered as representatives of the current stress regime, which has been approximately active for the last 800-1000 ka (Early-Middle Pleistocene). Recent activity of these faults is also indicated by faulted Late Pleistocene deposits (Cello *et al.*, 1997).

Data about micro- and meso-scale structural features (Angelier, 1984; Hancock, 1985) were collected to analyse the distribution of slip along the fault-traces and to reconstruct the paleostress field of the area (figs. 2 and 3). The fault-slip data set comprises slickenside lineations measured at 12 sites along the main fault-branches exposed in the area shown in figure 2, and at several minor outcrops. Slip data were collected on principal and auxiliary shear planes exposed on the face of bedrock fault-scarps or embedded in the gouge. Although secondary structural features related to the activity of the CEF and SMF fault-branches (dashed lines in fig. 2) affect Quaternary deposits of the Cesi basin (mainly tilted clay deposits), the intervening fault surfaces are very bad exposed and no measures regarding these faults were collected.

Two subsets have been selected from the entire data set. The first includes the population of meso-scale faults measured at several sites along the CFF. The second includes those along the CBF. Only measurements of certainly determined slip have been taken into account and slip observed at minor outcrops have been used only to verify the consistency of the entire data set. For these reasons, weights were kept equal to 1 in each data set in this analysis.

Reduced stress tensors were computed by direct inversion following the approach described by Angelier (1990) and using the program DAISY (Salvini, 1998). **The trend and plunge for σ_1, σ_2 and σ_3 (t1,p1;t2,p2;t3,p3) at CFF is (089,82;304,06;213,04), at CBF is (145,65;312,24;044,05) while the total is (119,84;297,06;027,00) with a ratio $\Phi=(\sigma_2-\sigma_3)/(\sigma_1-\sigma_3)$ respectively of 0.303, 0.448, 0.266.** Stereonet projection of fault slip data (fig. 3) exhibits a good fit between the distribution of the

observed slip and the computed shear stress. In addition, all the three solutions exhibit a shape ratio Φ that assumes low values (Φ~0.4) and show similar attitudes of the tension axis, suggesting a good level of homogeneity in the data set and indicating that the solutions are stable. Coherence among the solutions of the two subsets and the total data set enables us to deduce that the examined fault branches belong to the same generation of faults and, therefore, that the entire zone comprising the CFFS is controlled by a stress field which has a NE-SW striking tension axis with a slight sinistral component.

Seismological observations

Teleseismic observations showed that slip and moment centroid of the three M > 5.5 events are shallower than hypocentre depth (Olivieri & Ekström, 1999) thus implying an upward directivity of the sources. Because the slip is confined in the shallower portion of the crust, it is important to understand the possible relations between these earthquakes and their geological signature. To this purpose, we analysed **details of** fault geometry and kinematics of the three M > 5.5 events (see tab. 2 for a summary) and **localised** about 1000 M>2 events, **shown in figure 4,** among which 26 were M $\geq$ 4 (see tab. 1).

Three SSN local seismic networks operating in Umbria, Marche and Abruzzi regions, composed of 40 three–component short–period seismometers, and the ING network **(fig. 4)** provided digital recordings from September 3, 1997 onward. Up to 66 phase readings per event were accurately picked in a 110 Km radius circle around Colfiorito. This data set allowed locating M>2 events with enough accuracy on the horizontal plane (see next paragraph for a discussion of errors).

To compare the main ruptures to the exposed faults, it is important to assess depth distribution of such events. The favourable experimental framework and the availability of a velocity model (hereinafter P90) derived from deep seismic refraction studies in the area (Ponziani *et al.*, 1990), allowed us to give a reasonable estimate of hypocentral depths of most events.

In order to apply such detailed model (see fig. 5) to generic hypocentre location, the number of layers found in P90 has been reduced, joining two or more layers into one and assigning to the resulting layer an average velocity; such new simpler model shows a more uniform ray-path density in each layer. As the hypocentral depth of biggest events was about 8 km, the discontinuity that the model shows at such depth has been avoided by introducing a new interface at 4 km. Artificial clustering of hypocentres at 8 km has thus been reduced.

In order to utilise P90 in a complex tectonic environment such the CFFS, we have to take into account three-dimensional effects of the velocity structure, mainly due to a lateral lithological contrast

(Filippi & Alessandrini, 1999) and to the presence of Quaternary loose deposits. A trial and error procedure has been carried out to reduce RMS residuals by varying velocities and to evaluate static station corrections. In this way the use of a 3D velocity model is avoided to preserve location stability. The initial and the final models are shown in figure 5. We remark that we did not try to determine any new velocity model for the area, and that the procedure here applied only allowed the existing velocity model to be appropriate for hypocentre locations. Although a JHD technique would underline tectonic alignments, we did not attempt it because it was not needed for the purpose of this paper.

All events have been located by using the HYPOCENTER program (Lienert, Berg & Frazer, 1988). Phase readings weights have been established according to the reading uncertainty and to the hypocentral distance (weights have been assumed to be equal to 1 up to 40 km from the hypocentre, and then linearly decreasing, down to 0, with increasing distance up to 100 km). Outliers showing residuals greater than 1 s have been weighted out. The velocity model, the weighting criteria and the outliers removal threshold have been established on the basis of accurate analysis of the M≥4 events (listed in tab. 1), and then applied to the M<4 ones.

Initial solutions in the iterative location procedure have been chosen according to the «S-P solution» on the horizontal plane and in accordance to the behaviour of the RMS versus depth. Location errors have been computed by using the standard procedure of HYPOCENTER (Lienert *et al.*, 1988) and then verified for the M>5.5 events, following the approach discussed by Di Giovambattista & Barba (1997).

~~A summary of hypocentral parameters,~~ Source kinematic properties (Zollo *et al.*, 1998; 1999) for the three M>5.5 events are listed in table 2 and represented in figure 6. Depths of major events (no. 2, 3 and 18) is compatible with those estimated by strong motion accelerometer data (Zollo *et al.*, 1999) in the limit of measurement errors. Earthquake locations are shown in vertical sections in figures 7 and 8.

On the influence of measurement errors

Standard procedures of instrumental data inversion are usually affected by several sources of errors that in turn affect interpretations. In this section, we will evaluate the influence of location errors, on the horizontal and vertical planes (tab. 1), and of the uncertainties associated to the source parameters onto our results.

~~Errors on the horizontal plane~~

We derived which faults could have been reactivated during the earthquake swarm from the epicentre distribution (fig. 4), assuming that a SW dipping normal fault can be probably considered

active if such fault **delineates** the seismicity distribution. Since the spacing between the mapped normal faults is much greater than the earthquake location errors on the horizontal plane, interpretations based on earthquake locations will not change by varying epicentres within the measurement errors.

~~**Errors on the vertical plane**~~

~~Uncertainties on depth of M≥5.5 earthquakes instead are crucial when comparing modelled fault planes to geologically surveyed faults.~~ In order to better constrain depths of M>5.5 earthquakes we ~~took into account strong motion modelling by using results of Zollo *et al.* (1999) as initial values and~~ evaluated the influence of different initial depths on final ones. The good geometry of the network (gaps lower than ~60° for M>5.5) and the condition that the final solution was close to the one inferred by strong motion analysis **(Zollo *et al.*, 1999)** allowed errors of +/-1 km~~; those errors can probably represent the lower limit admitted by standard location techniques in such well constrained cases~~. To address the influence that errors associated to arrival times and to the velocity model have on depth, we used the method of Di Giovambattista & Barba (1997)~~ has been applied to M≥5.5 events and to a few M>4 (tab. 2) events~~ and concluded that depth uncertainties **are unvarying** from NW to SE of Colfiorito. This observation supports conclusions based on the differences in the average depth from NW to SE. Smaller earthquakes (M≤5.5) have been considered to be affected by standard errors~~, after some testing as described later. Therefore~~ **and** depth values of any specific M≤5.5 earthquake was never used to draw any conclusion. Only the average behaviour of low magnitude seismicity with regard to its depth has been taken into account. As an example, the deepening of seismicity toward SW (fig. 7) or toward NW (fig. 8b) from the Colfiorito fault can be considered as «average behaviour».

~~**Errors on source parameters**~~

To evaluate **empirical** errors on source **properties we** compared results drawn by completely different approaches~~ could help assess uncertainties otherwise hard to be estimated~~. The kinematic model (Zollo *et al.*, 1998; 1999) and the **static model** ~~source parameters derived by~~ (Hunstad *et al.*, 1998)~~, based upon estimation of coseismic deformations, one could find~~ **show** a difference of +/- 2 km in fault width~~ (respectively 6 km vs. 8 km in the evaluation of fault no. 2)~~ **that** does not change conclusions on which fault plane ruptured. Moreover, ~~differences between solutions in slip distribution on the fault depend only on the data constraints, and do not depend on the underlying theory. In particular,~~ both works state that the maximum slip is modelled to be in the first segment of the fault no. 3~~; with regards to faults no. 2 and no. 18, while Zollo *et al.* (1998, 1999) and Stramondo *et al.* (1999) allow greater detail in describing the slip distribution than those obtainable from Hunstad *et al.* (1998), that assume uniform slip distribution over such faults. A summary of hypocentral parameters and~~

~~source properties utilised in this work is shown in table 2~~. **The slip distribution along fault inferred from Zollo's (1999) work is shown in figure 9.**

Errors discussed in this section do not change the conclusions drawn from the results.

Earthquake geological effects

In this section we adopt and review the descriptions of geological effects reported in Basili *et al.* (1998), that result from field surveys that were carried out just after the various earthquakes. We also summarise the criteria used to determine whether the faults broke the ground surface and to assess types and size of surface deformation.

Apart from the typically gravity-controlled deformations, such as landslides and associated features that were scattered all over the surveyed area two main different types of surface brittle deformation were detected. The first type (A) consists of offsets between bedrock and slope deposits which occurred in correspondence of possibly reactivated faults. This type of deformation was eventually interpreted as having been induced by ground shaking and clearly controlled by gravity. The second type (B) is that of tectonically originated ruptures which consists of coseismic displacements of bedrock. Secondary cracks and fissures have also been observed but are beyond the purpose of this analysis.

Normal fault slip vectors have the peculiarity of being concordant to the gravity vector. Therefore, having both types of surface brittle deformation occurred in correspondence of possibly re-activated normal faults the distinction between type A and type B was not straightforward. Qualitative criteria relying on mechanical properties of rocks and soft-sediments, geomorphologic characteristics of the sites, structural features, and kinematic indicators were thus applied to discriminate one type from the other.

Features induced by ground shaking (type A) occurred after the two first mainshocks (earthquakes nos. 2 and 3) along the CFF, MTF and COF fault-scarp and exhibited the following characteristics: (i) displacement length was a very small portions of total fault length (3%); (ii) displacements were detected only at the contact between bedrock and slope deposits and soft-sediments; (iii) no displacement was ever detected where bedrock is exposed on both walls of the fault; (iv) no displacement were detected where the ground flattens; (v) slip features followed the contact between bedrock and slope deposits even where the fault-scarp is retreated; (vi) there was always accordance between slip vector and maximum slope direction; (viii) slip vector was maximum on topographic highs and minimum (tends to zero) in topographic lows; (ix) slip vectors **measured** across **narrow** stream incisions **had opposite directions**.

Conversely, features ascribed to type B occurred in the southern area after the third mainshock (earthquake no. 18). Although no faults were previously mapped in this area, on the Col Beccariccio SW slope a bedrock fault-scarp is clearly exposed and is aligned toward SE with the co-seismic ruptures (see CBF and RRM in fig. 6). Tectonic features found along the RRM lineament exhibited the following characteristics: (i) ruptures cut across the surface regardless of the local morphology; (ii) ruptures cut through the rocks regardless of their mechanical properties; (iii) ruptures were mostly continuous; (iv) ruptures exhibited coherent meso-scale structural features; (v) coseismic slip, inferred by composing vectors of maximum vertical and horizontal displacements, pitched at about 60° to the SE in good accordance to the CBF slickenside lineations.

A summary of the observed offsets versus fault strike is plotted in the diagrams of figure 10.

Discussion

The CFFS belongs to a complex geodynamic framework that includes an active W plunging subduction driving an East oriented orogenic **progression** with a consequent crustal extension in the rear that dominates the tectonic style of the region. In this framework major earthquakes may occur where the easternmost normal faults of the Apennines record Pleistocene-Holocene tectonic activity. Numerical modelling of the stress pattern in this region shows that insights of fault behaviour and their correlation with local seismicity are needed to produce reliable models of long-term (inter-seismic) tectonic stress accumulation (Negredo *et al.*, 1999). Such analysis would help predict location, geometry and mechanism of major earthquake faulting.

The 1997-98 Colfiorito seismic swarm is an intriguing example in this perspective. In fact, the complex geologic structure of the CFFS (fig. 2) includes several individual small-size faults **that are difficult to** correlate to the seismogenic sources. Unfortunately, surface geological effects that occurred on the various branches of the CFFS and in the surrounding areas were very different in nature and mechanism and their analysis resulted in dissimilar interpretations and deductions (see for example Basili *et al.*, 1998; Cello *et al.*, 1998; Cinti *et al.*, 1999).

~~The analysis presented in the previous sections provides several issues, discussed below, which contribute in shading some light in understanding the role of each fault-branch pertaining to the CFFS.~~

Considering the position of the mainshock hypocentres (figs. ~~7~~**6** and ~~8~~**7**) and source-fault properties (tab. 2) it seems very likely that earthquakes nos. 1, 2, 3, and probably no. 4, originated on the same structure **and produced blind normal faulting with ruptures stopping at ~4 km below the ground surface (figs. 7 and 8).** ~~being the geometrical uncertainties among the modelled fault-planes as small as those that could be found in modelling a single fault.~~ **Given the errors of 1.1 Km on hypocentral depth (event no. 3 in tab. 1), the uncertainty of ~2 Km in fault width, and the**

indeterminacy of the fault plane dip of ±14° associated to CMTs (Helffrich, 1997), the top edge of the fault has to be deeper than 500 m below the ground surface. ~~Fault plane solutions for these earthquakes require blind normal faulting with ruptures stopping at ca. 4 km below the ground surface.~~ **Differently, earthquake** no. 18 originated on another structure, and the fault plane solution for this earthquake requires normal faulting with coseismic rupture stopping at about 2 km below the ground surface. **Taking into account errors as above, it is possible that the fault no. 18 intersects the ground surface.**

These arguments support the following interpretation of geological effects. Earthquakes nos. 1-4 did not break the surface and the offsets between bedrock and slope deposits observed along the correlative fault-scarps should be interpreted as an effect of ground-shaking. **This suggests a slip-rate strengthening behaviour of the CFF gouge (Marone and Scholz, 1988) supported also by the strong decrease of seismicity at the upper transition from high- to low-velocity layers (~1.5–3 km).** Conversely, considering the errors associated to the solution of earthquake no. 18, the surface ruptures observed along the RRM alignment could be interpreted either as surface faulting or as brittle accommodation of an extensional forced fold.

Kinematic properties of earthquakes nos. 1-4 and 18 provides an estimation of subsurface fault length, down-dip width and directivity (tab. 2 and fig. 6). As observed in large size earthquakes early aftershocks well define the dimension of the mainshock fault planes as well as late aftershocks define the total ruptured volume of rock (e.g. Dietz & Ellsworth, 1990; Richins *et al.*, 1987). Likewise, in this case of moderate size earthquakes the mainshock fault-plane mostly overlap the distribution of early aftershocks (fig. 8a) independently confirming the estimated subsurface dimension of the fault.

The aftershock distribution across strike plunges south-westward (cross-sections, fig. 7) in accordance to the predicted fault-dip, and is bordered by the projections to depth of the surveyed fault planes (fig. 4). The aftershock depth distribution along strike (longitudinal section, fig. 8) becomes thinner from NW to SE, in accordance with depth distribution of the mainshocks, and shows that much of the accompanying deformation in the south-eastern area is located near the ground surface. ~~In addition it is worth noting that a series of events with M≥4 (nos. 11, 12, 13, 14, 17, 19), which occurred between the 10-15 October 1998, probably reactivated the CBF which is well aligned with the RRM ruptures. Therefore, the other fault planes of the system (CEF, COF and MTF) could have been reactivated only by minor events.~~ We observe also that the dimension along strike of the deformed volume of rock is by far greater than the total subsurface length of the mainshock fault planes and, in turn, of the faults exposed at the ground surface.

The above observations are consistent with the reactivation at depth of **relatively steep (~40°)** fault planes ~~connecting the foci of earthquakes nos. 1-4~~ related with the **clearly steep outcropping**

planes of the CFFS. ~~and the focus of earthquake no. 18 related with the RRM coseismic ruptures,~~ These are the nearest geological structures to the east of the source fault top edges among the easternmost principal normal faults in the region.

The average strain field derived from slickenside lineations analysis (fig. 3) seems to be strictly correlated to the ~~dynamic stress~~ **strain** field deduced from the earthquake focal mechanisms of the three main events (tab. 2) suggesting a possible correlation between the growth of the CFFS over geological time (since Early-Middle Pleistocene) and its coseismic behaviour.

The slip distribution along the combined fault related to events nos. 2 and 3 (fig. 9) has a maximum in the central sector of the total ruptured area which corresponds to the best exposed portion of the CFF and also to the most lowered portion of the hanging-wall topographic relief (fig. **6**). As such the slip distribution observed during earthquakes nos. 2 and 3, that represents the most part of the total slip of the swarm, could be related to the long term cumulative subsidence of the Colfiorito Basin. ~~If such is the case, then the length of rupture at depth could represent the total length of a fault that is still growing at the surface.~~

The similarity between the coseismic slip and the long term cumulative displacement would likely indicate a seismogenic source producing **1997-like** earthquakes. In any case, if faults 1-4 would interact fracturing as a single structure, a maximum magnitude M_S=6.4 (Utsu & Seki, 1954) **and a slip distribution similar to 1997 ruptures** would be expected. ~~A consistent model that relates geological structure characteristics to the subsurface rupture dimension in regions of moderate size earthquakes is unfortunately not yet available posing compelling questions upon how the geological study of exposed faults should be directed to help assess seismic hazard~~.

Conclusions

We analysed and combined the results of geological and seismological observations of the 1997 Umbria-Marche earthquake swarm. We explored the relationships between the structural features detected by geological field surveys and the mainshock fault-planes (M > 5.5) modelled by seismological recordings. The low magnitude seismicity played an essential role in the interpretation by constraining dimension and location of the deformed volume of rock.

Although earthquakes nos. 1-3 seem to have reactivated an already mapped active normal fault (CFF), no surface faulting was detected along its trace. In the case of earthquake no. 18, tectonic ruptures (RRM) due to either surface warping or possibly surface faulting occurred in an area where pre-existing normal faults were neither mapped nor clearly visible in the field.

The total length of the normal faults exposed in the area is about 2/3 of the subsurface maximum fault length predicted by the instrumental data. However, the best exposures of the fault in the field

and their associated geological structures occur in accordance with the slip distribution derived from the source kinematics~~ if self-similar behaviour of the fault could be assumed in a long-term perspective~~.

~~The problems dealt with the interpretation of these earthquakes represent typical and widespread examples for the Italian peninsula and for other regions of the Earth characterised by a low seismicity level. Therefore, in order to give a thorough interpretation of a moderate-sized earthquake and its related processes, including geological surface effects and deformation pattern, it is strongly recommended that seismological and geological data be accurately combined.~~

The test case of the Colfiorito Fault System offered a unique opportunity to study the mechanisms related to the retreat and bending of a W-plunging subduction~~ and showed that low magnitude seismicity improved the analysis of this particular seismic crisis.~~ The good accordance between the reduced stress tensor derived from fault plane kinematic indicators and the observed mainshock focal mechanisms suggests a long-term persistence and coaxiality condition of the regional strain field. This fact allows us to consider the same earthquake generating mechanism being probably active since Early-Middle Pleistocene and supports the use of data analysed in this work in constraining tectonic models. Therefore, we expect that the analysis of long-term structures that could be associated to low-magnitude seismicity would improve, at least in well known fault systems, our understanding of long term tectonic stress loading.

Acknowledgements

Seismometric data were supplied by ING and SSN, while geological field survey was supported by IRTR-CNR (GNDT project). C. Doglioni, S. Ward, and R. Sabadini are acknowledged for useful discussions. A. Zollo is thanked for giving us his results before publication. Comments made by George Helffrich and an anonymous reviewer improved the manuscript.

References

Amato, A., Azzara, R., Chiarabba, C., Cimini, G.B., Cocco, M., Di Bona, M., Margheriti, L., Mazza, S., Mele, F., Selvaggi, G., Basili, A. Boschi, E., Corboulex, F., Deschamps, A., Gaffet, S., Bittarelli, G., Chiaraluce, L., Piccinini, D. & Ripepe, M., 1998. The 1997 Umbria-Marche, Italy, earthquake sequence: a first look at the main shocks and aftershocks. *Geophys. Res. Lett.*, **25**, 15, 2861-2864.

Angelier, J., 1984. Tectonic Analysis of Fault Slip Data Sets. *J. Geophys. Res.*, **89**, B7, 5835-5848.

Barba, S., Di Giovambattista, R. & Smriglio, G., 1995. Accessing the Istituto Nazionale di Geofisica Seismic Network Databank (ISDN). *EOS*, **76**, 9, 28/02/1995.

Barchi, M., Minelli, G. & Pialli, G., 1997. The Crop 03 profile: a synthesis of results on deep structures of the Northern Apennines. In: Pialli G., Barchi M. & Minelli G. (Eds), 1998, Results of the CROP03 deep seismic reflection profile. *Mem. Soc. Geol. It.*, **52**, 383-400.

Basili, R. & Meghraoui, M., 1999. Coseismic and postseismic displacements related with the 1997 Umbria-Marche (Italy) earthquake sequence. *Geophysical Research Abstracts*, **1**(1), 95.

Basili, R., Bosi, V., Galadini, F., Galli, P., Meghraoui, M., Messina, P., Moro, M. & Sposato, A., 1998. The Colfiorito earthquake sequence of September-October 1997: Surface breaks and seismotectonic implications for the central Apennines (Italy), *Journal of Earthquake Engineering*, **2**, 291-302.

Berardi R. & ENEL S.M. network working group, Marsan P. & SSN seismic monitoring working group, Deschamps A. & Geoazur-CNES research group, Di Bona M. & ING research group, Rinaldis D. & ENEA S.M. network working group, 1998. Strong ground motion during the 1997 Umbria-Marche earthquake sequence (abstract). *Annales Geophysicae*, **16**, suppl. 1.

Boncio, P., Ponziani, F., Brozzetti, F., Barchi, M., Lavecchia, G. & Pialli, G., 1997. Seismicity and extensional tectonics in the northern Umbria-marche Apennines, *Mem. Soc. Geol. It.*, 52, 539-555.

Bonilla, M.G., 1988. Minimum earthquake magnitude associated with coseismic surface faulting, *Bull. Assoc. Eng. Geologists*, **25**, 17-29.

Bonilla, M.G., Mark, R.K., & Lienkaemper, J.J., 1984. Statistical relations among earthquake magnitude, surface rupture lenght, and surface fault displacement. *Bull. Seism. Soc. Am.*, **74**, 2379-2411.

Boschi, E., Ferrari, G., Gasperini, P., Guidoboni, E., Smriglio, G. & Valensise, G., 1997. *Catalogo dei forti terremoti in Italia dal 461 a.C. al 1990* (in Italian). Istituto Nazionale di Geofisica, Rome, Italy, 973 pp.

Bosi, C., Coltorti, M. & Dramis, F., 1983. Carta del Quaternario della conca di Gualdo Tadino. Unpublished map, CNR-CSGT and Min. Pubbl. Istr., Progetto Morfoneotettonica, Rome.

Calamita, F. & Pizzi, A., 1992. Tettonica quaternaria nella dorsale appenninica umbro-marchigiana e bacini intrappenninici associati. *Studi Geol. Cam.*, spec. vol. **92/1**, 17-25.

Camassi, R., Galli, P., Molin, D., Monachesi, G. & Morelli, G., 1997. Rilievo macrosismico preliminare del terremoto umbro-marchigiano di settembre-ottobre 1997. *Ingegneria sismica*, **6/97**, 4, 50-54.

Cattaneo, M., De Luca, G., Gorini, A., Michelini, A., Monachesi, G., Ponziani, F. & XGUMS (eXperimental Group for Umbria-Marche Seismicity), 1998a. Umbria-Marche earthquake sequence: the contribution of the Umbria, Marche and Abruzzo local seismic networks. A*nnales Geophysicae*, **16**, suppl. 1.

Cattaneo, M., Michelini, A., Milana, G. & XGUMS (eXperimental Group for Umbria-Marche Seismicity), 1998b. Umbria-Marche earthquake sequence: the GNDT-UNIGE/OGS-DINMA and SSN seismic network. *Annales Geophysicae*, **16**, suppl. 1.

Cello, G., Deiana, G., Mangano, P., Mazzoli, S., Tondi, E., Ferreli, L., Maschio, L., Michetti, A. M., Serva L. & Vittori E., 1998. Evidence for surface faulting during the September 26, 1997, Colfiorito (Central Italy) earthquakes. *Journal of Earthquake Engineering*, **2**, 303-324.

Cello, G., Mazzoli, S., Tondi, E. & Turco, E., 1997. Active tectonics in the central Apennines and possible implications for seismic hazard analysis in peninsular Italy, *Tectonophysics*, **272**, 43-68.

Cinti, F., Cucci, L., Marra, F. & Montone, P., 1999. The 1997 Umbria-Marche (Italy) earthquake sequence: Relationship between ground deformation and seismogenic structure. *Geophys. Res. Lett.*, **26**, 895-898.

Coltorti, M. & Dramis, F. 1988. The significance of slope-waste deposit in the Quaternary of Umbria-Marche Apennines, Central Italy. Zeit. Geomorph., N.F. Suppl., 71, 59-70.

De Martini, P. M., Marchioni, A. & Valensise, G., 1999. Modelling of elevatioon changes induced by the 1997-98 Umbria-Marche earthquakes: further evidence for shallow-angle normal faulting. *Geophysical Research Abstracts*, **1**(1), 95.

Deschamps, A., Iannaccone, G. & Scarpa, R., 1984. The umbrian earthquake (Italy) of 19 September 1979, *Annales Geophysicae*, **2**, 1, 29-36.

Di Giovambattista, R. & Barba, S., 1997. An estimate of hypocenter location accuracy in large network: possible implications for tectonic studies in the Italian case. *J. Geoph. Int.*, **129**, 4.

Dietz, L.D. & Ellsworth, W.L., 1990. The October 17, 1989, Loma Prieta, California, earthquake and its aftershocks: geometry of the sequence from high-resolution locations. *Geophys. Res. Lett.*, **17**, 1417-1420.

Doglioni, C., 1997. Italy (Sections: Regional geology; Tectonics). In: E. M. Mooores and R. W. Fairbridge, eds., Encyclopedia of European and Asian Regional Geology. Chapman & Hall, London, UK., p.414-435.

Doglioni, C., Mongelli, F. & Pialli, G., 1997. Boudinage of the Alpine belt in the Apenninic back-arc. In: Pialli G., Barchi M. & Minelli G. (Eds), 1998, Results of the CROP03 deep seismic reflection profile. *Mem. Soc. Geol. It.*, **52**, 457-468.

Dziewonski, A.M. & Woodhouse, J.H., 1983. Studies of the seismic source using normal-mode theory, in Kanamori, H. and E. Boschi, eds., Earthquakes: observation, theory, and interpretation: notes from the International School of Physics "Enrico Fermi" (1982: Varenna, Italy), North-Holland Publ. Co., Amsterdam, pp. 45-137.

Ekström, G., Morelli, A., Boschi, E. & Dziewonski, A. M., 1998. Moment tensor analysys of the Umbria-Marche earthquake sequence of September-October 1997. *Geophys. Res. Lett.*, **25**, 11, 1971-1974.

Ficcarelli, G., Abbazzi, L., Albianelli, A., Bertini, A., Coltorti, M., Magnatti, M., Masini, F., Mazza, P., Mezzabotta, C., Napoleone, G., Rook, L., Rustioni, M. & Torre, D., 1997. Cesi, an early Middle Pleistocene site in the Colfiorito Basin (Umbro-Marchean Apennine), central Italy. *J. Quaternary Sc.*, **12**, 507-518.

Filippi L. & Alessandrini B., 1999. Upper-crustal structure of Central Apennine (Italy) from local earthquakes. Submitted to *Tectonophysics*.

Haessler, H., Gaulon, R., Rivera, L., Console, R., Frogneux, M., Gasparini, C., Martel, C., Patau, G., Siciliano, M. & Cisternas, A., 1988. The Perugia (Italy) earthquake of 29 April 1984: a microearthquake survey, *Bull. Seism. Soc. Am.*, **78**, 6, 1948-1964.

Hancock, P.L., 1985. Brittle microtectonics: principles and practice. *J. Structural Geol.*, **7**, 437-457.

Hunstad, I., Anzidei, M., Baldi, P., Galvani, A. & Pesci, A., 1988. Gps observations of co-seismic displacement of the Umbria-Marche seismic sequence. *Annales Geophysicae*, **16**, suppl. 1.

Lienert, B.R., Berg, E. & Frazer, L.N., 1988. HYPOCENTER: An earthquake location method using centered, scaled, and adaptively least squares. *Bull. Seism. Soc. Am.*, **76**, 771-783.

Marone, C. & Scholz, C. H., 1988. The depth of seismic faulting and the upper transition from stable to unstable slip regimes. *Geoph. Res. Letters*, **15**, 621-624.

Menichetti, M., 1992. Evoluzione tettonico-sedimentaria della valle di Gubbio. *Studi Geologici Camerti*, spec. vol. 92/1, 155-163.

Meghraoui, M., Bosi, V. & Camelbeeck, T., 1998. Fault fragment control in the 1997 Umbria-Marche, central Italy, earthquake sequence. *Geoph. Res. Letters*, **26**, 1069-1072.

Negredo, A. M., Carminati, E., Barba, S. & Sabadini, R., 1999. Numerical modelling of the stress accumulation and seismotectonics in central Italy. *Geophys. Res. Lett.*, **26**, 1945-1948.

Olivieri M. & Ekström, G., 1998. Rupture depths and source processes of the 1997-1998 earthquake sequence in central Italy. *Bull. Seism. Soc. Am.*, **89**, 305-310.

Pialli, G., Barchi, M. & Menichetti, M., 1991. Studi preliminari all'acquisizione dati del profilo CROP 03 Punta Ala-Gabicce, *Studi Geologici Camerti*, Spec. Vol., 1, 463 p.

Pino, N. A., Mazza, S. & Boschi, E., 1999. Rupture directivity of the major shocks in the 1997 Umbria-Marche (Central Italy) sequence from regional broadband waveforms. *Geoph. Res. Lett.*, **26**, 2101-2104.

Ponziani, F., De Franco, R., Minelli, G., Biella, G., Federico, C. & Pialli, G., 1990. Crustal shortening and duplication of the Moho in the Northern Apennines: a view from seismic refraction data. *Tectonophysics*, **252**, 391-418.

Richins, W.D., Pechmann, J.C., Smith, R.B., Langer, C.J., Goter, S.K., Zollweg, J.E. & King, J.J., 1987. The 1983 Bora Peak, Idaho, earthquake and its aftershocks. *Bull. Seism. Soc. Am.*, **77**, 694-723.

Salvini, F., 1998. The Structural Data Integrated System Analyzer, Version 2.151b, 27/10/98. Dip. Scienze Geologiche, Univ. Roma TRE, Rome, Italy.

Stramondo, S., Tesauro, M., Briole, P., Sansosti, E., Salvi, S., Lanari, R., Anzidei, M., Baldi, P., Fornaro, G., Avallone, A., Buongiorno, M.F., Franceschetti, G. & Boschi, E., 1999. The September 26, 1997 Central Italy earthquakes: coseismic surface displacement detected by SAR interferometry and GPS, and faulting modeling. *Geophys. Res. Lett.*, **26,** 883-886.

Utsu T. & Seki A., 1954. A relation between the area of aftershock region and the energy of main shock, *J. Seismol. Soc. Jpn.*, **7**, 233-240.

Wells, D.L. & Coppersmith, K.J., 1994. New Empirical Relationships among Magnitude, Rupture Lenght, Rupture Width, Rupture Area, and Surface Displacement, *Bull. Seism. Soc. Am.*, **84**, 974-1002.

Zollo, A., Bongiovanni, G., Herrero, A., Marcucci, S. & Milana, G., 1998. The 1997 Colfiorito Earthquake sequence (Central Italy): insights on mainshock ruptures from near source strong motion records (abstract). *Annales Geophysicae*, **16**, suppl. 1.

Zollo, A., Marcucci, S., Milana, G. & Capuano, P. 1999. The 1997 Umbria-Marche (Central Italy) earthquake sequence: Insights on the mainshock ruptures from near source strong motion records. *Geoph. Res. Lett.*, **26**, 20, 3165-3168.

Figure Captions

Fig. 1 - Sketch-map showing extensional (dashed line) and compressional zones (dotted line) within the northern Apennine chain. Light-grey rectangle (enlarged in subsequent figures) contains earthquakes analysed in this paper. CMT solutions after Harvard catalogue (Dziewonski & Woodhouse, 1983). http://www.seismology.harvard.edu/CMTsearch.html

Fig. 2 - Sketch-map of the area struck by the Colfiorito earthquakes showing the CFFS, the drainage network, the main Quaternary basin deposits (grey), and location of mainshocks listed in table 1.

Fig. 3 - a) Stereographic projections of fault slip data measured along the main fault-branches exposed in the area shown in figure 2 and at several minor outcrops; **principal stress axes are also shown.** b) Distribution of average slip data along strike on the CFFS (black arrows), and slip of the RRM surface ruptures (grey arrows).

Fig. 4 – Map view of the 1997 Colfiorito swarm. Dark-grey circles: M>5.5; light-grey circles: M≥4 (recorded between 09/03/97 and 12/31/97); small white circles: M>2 (recorded between 09/28/97 and 12/31/97). **Triangles represent SSN and ING seismometers that provided at least one phase reading.**

Fig. 5 - Velocity model used to localise all events analysed here. P90 refers to the model derived by Ponziani *et al.* (1990). Vp/Vs=1.9 is assumed to be constant.

Fig. 6 – Map of the earthquake area. Contours from a digital elevation model (grid 230x230 m). Fault plane solutions after Zollo *et al.* (1999) have been projected on the surface in dark grey with isodepths. The arrows indicate source directivity, according to strong motion data from SSN.

Fig. 7 – Projections of the fault-plane solutions and fault outcrops on SW-NE sections (a) across the CFF (A–A') and (b) across the CBF-RRM (B–B'). Cross-section traces and selection boxes are shown in figure 4.

Fig. 8 - Longitudinal section C-C': (a) early aftershocks of the September 26, 1997, recorded by SSN temporary network before October, 3rd 1997; (b) all aftershocks already shown in figure 4.

Fig. 9 - Slip distribution along fault for the 00:33 (right) and 09:40 (left) events obtained by multiplying the source time functions (at a station in Assisi) by the estimated rupture velocity (Zollo *et al.*, 1999) and projecting the derived slip history along the directivity unit vector.

Fig. 10 - Distribution along strike (NW-SE) of (a) the offset between bedrock and slope deposits for the CFF, COF, MTF, and CBF fault-branches and of (b) the displacement between bedrock walls for the RRM ruptures.

Table Captions

Tab. 1 - List of M≥4 earthquake solutions. Magnitudes M_L, M_W or M_D; are labelled respectively with L, W, D (M_L and M_D from ING; M_W from Ekström *et al.*, 1998). The magnitude of event no. 4 is not determinable from our records, because of the coda of earthquake no. 3. A rough estimate of that magnitude indicates a value of about M≈5 taking also into account the damage caused by such earthquake and reported by P. Galli (personal communication).

Tab. 2 - Summary of source properties of M_W>5.5 events (no. 2 and 3 taken from Zollo, 1999; no. 18 from Zollo, 1998). L: fault length along strike; W: width along dip; V_R: rupture velocity. Note that the bottom of the fault plane coincides with the focal depth.

Table 1

Event No.	Date	Origin time (GMT)	Lat	Long	Depth (km)	Mag	No. obs.	Gap	Rms (s)	Erh (km)	Erz (km)
1	970903	22:07:29.83	43°00.99	12°50.80	9.1	4.5 W	37	158	0.23	0.9	0.6
2	970926	00:33:12.89	43°01.38	12°52.42	7.0	5.7 W	58	42	0.30	0.7	0.9
3	970926	09:40:26.73	43°01.78	12°50.09	8.0	6.0 W	42	33	0.32	1.0	1.1
4	970926	09:47:38.29	43°06.18	12°47.38	7.2	Unk	22	199	0.23	1.5	1.7
5	970926	13:30:52.45	43°00.92	12°54.37	6.1	4.5 W	30	125	0.29	1.1	1.1
6	970927	08:08:07.93	43°06.50	12°48.12	5.6	4.3 L	33	89	0.22	0.6	0.9
7	970927	19:56:43.38	43°03.29	12°50.88	5.8	4.0 L	42	65	0.25	0.6	0.8
8	970928	11:24:31.91	42°58.64	12°50.77	4.0	4.0 L	36	105	0.28	0.9	1.0
9	971002	10:59:56.27	43°05.86	12°46.34	6.5	4.1 L	72	36	0.27	0.5	0.5
10	971003	08:55:22.02	43°01.95	12°49.90	5.7	5.2 W	68	43	0.28	0.5	0.7
11	971004	06:49:59.49	42°55.43	12°54.39	5.9	4.1 D	66	88	0.22	0.5	0.6
12	971004	15:07:21.01	42°55.80	12°54.81	6.1	4.2 L	73	57	0.27	0.5	0.6
13	971004	16:13:32.97	42°55.84	12°55.25	3.5	4.7 W	71	56	0.34	0.7	0.7
14	971004	18:47:47.87	42°55.62	12°56.06	3.5	4.1 L	64	57	0.23	0.5	0.8
15	971006	23:24:53.23	43°00.76	12°49.79	7.4	5.4 W	70	46	0.24	0.5	0.5
16	971007	05:09:57.03	43°01.54	12°50.84	6.4	4.5 W	71	68	0.22	0.5	0.6
17	971012	11:08:36.87	42°54.13	12°56.10	2.6	5.2 W	60	61	0.35	0.7	0.7
18	971014	15:23:10.61	42°54.11	12°54.75	5.5	5.6 W	66	61	0.29	0.8	1.0
19	971015	22:53:10.78	42°55.39	12°55.59	5.6	4.1 L	64	86	0.24	0.5	0.6
20	971016	04:52:55.66	42°56.23	12°54.75	2.1	4.3 W	61	80	0.20	0.4	0.4
21	971016	12:00:31.54	43°02.81	12°52.92	5.6	4.5 L	71	46	0.46	0.8	1.1
22	971019	16:00:17.59	42°58.13	12°51.18	6.9	4.2 W	92	46	0.23	0.4	0.4
23	971020	01:27:04.93	42°59.35	12°52.27	6.1	3.8 D	94	44	0.22	0.4	0.5
24	971025	03:08:06.15	42°49.14	13°04.43	2.2	3.9 D	90	25	0.28	0.4	0.4
25	971109	19:07:33.67	42°51.71	12°59.59	3.0	4.6 D	59	93	0.43	0.8	0.8
26	971231	16:02:15.60	42°50.69	13°01.61	7.7	4.0 D	31	94	0.46	1.4	1.7

Table 2

Evt No.	Strike	Dip	L (Km)	W (Km)	V_R (Km/s)
2	[b]148°	[b] 36°	[b] 6	[b] 6	[b] 3
3	[b]152°	[b] 38°	[b] 12	[b] 7.5	[b] 2.6
18	[a]144°	[a] 40°	[a] 6	[a] 6	

Fig. 1

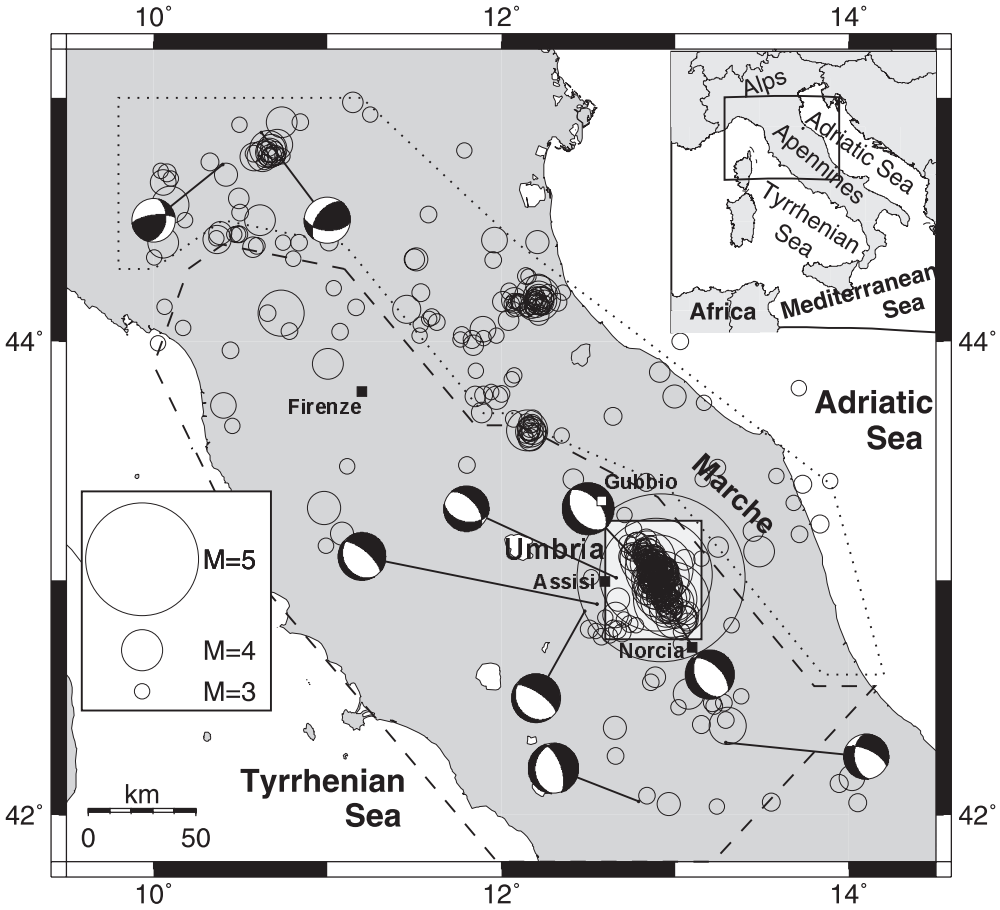
10˚
12˚
14˚
44˚
42˚
Alps
Adriatic Sea
Apennines
Tyrrhenian Sea
Africa
Mediterranean Sea
Firenze
Adriatic Sea
Gubbio
Marche
Umbria
Assisi
Norcia
M=5
M=4
M=3
km
0
50
Tyrrhenian Sea

Fig. 2

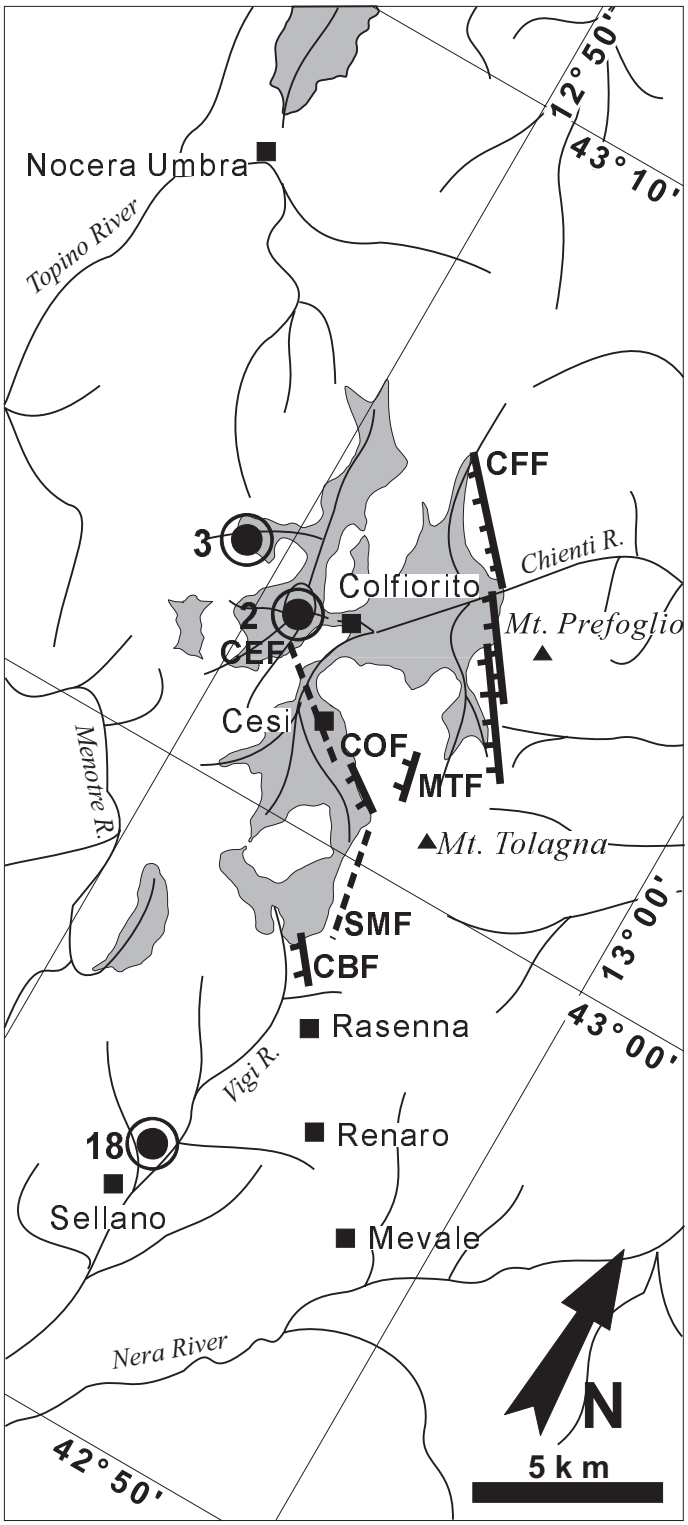
Nocera Umbra
Topino River
12° 50'
43° 10'
CFF
3
Chienti R.
Colfiorito
2
Mt. Prefoglio
CEF
Cesi
COF
MTF
Menotre R.
Mt. Tolagna
SMF
CBF
13° 00'
43° 00'
Rasenna
Vigi R.
18
Renaro
Sellano
Mevale
Nera River
42° 50'
N
5 k m

Fig. 3

a)

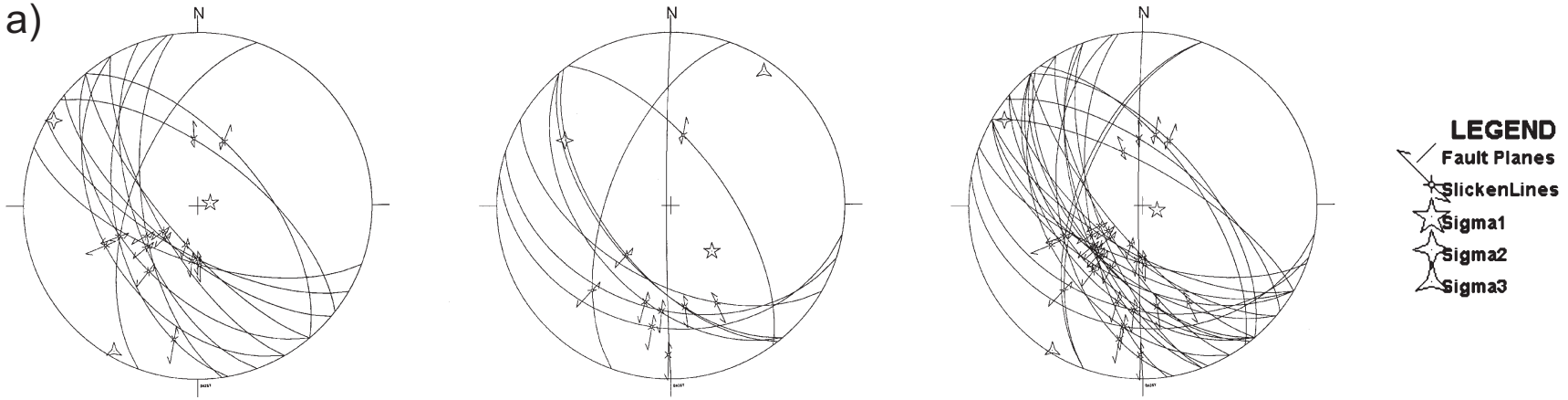

CFF **CBF** **TOTAL**

b)

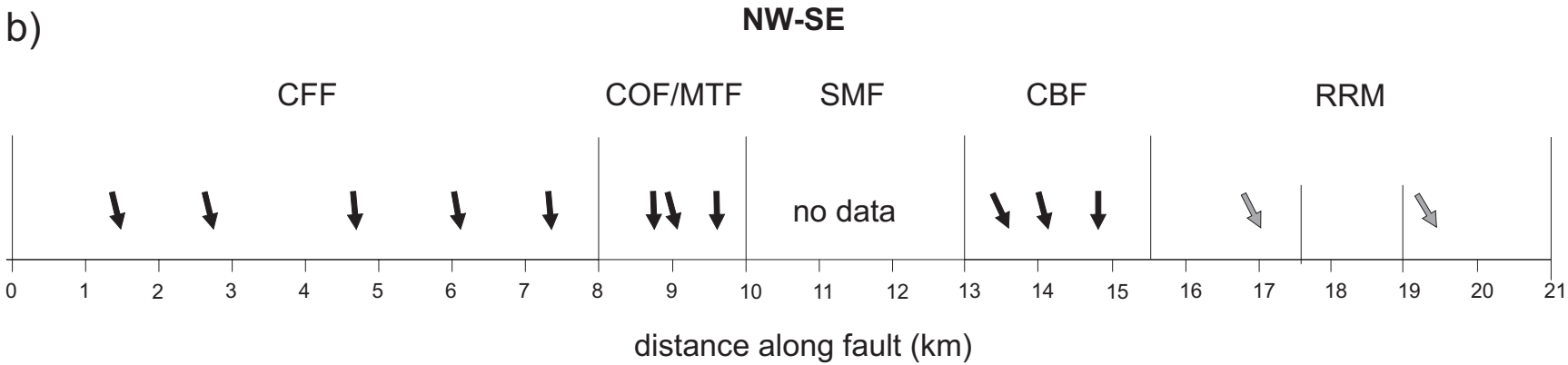

Fig. 4

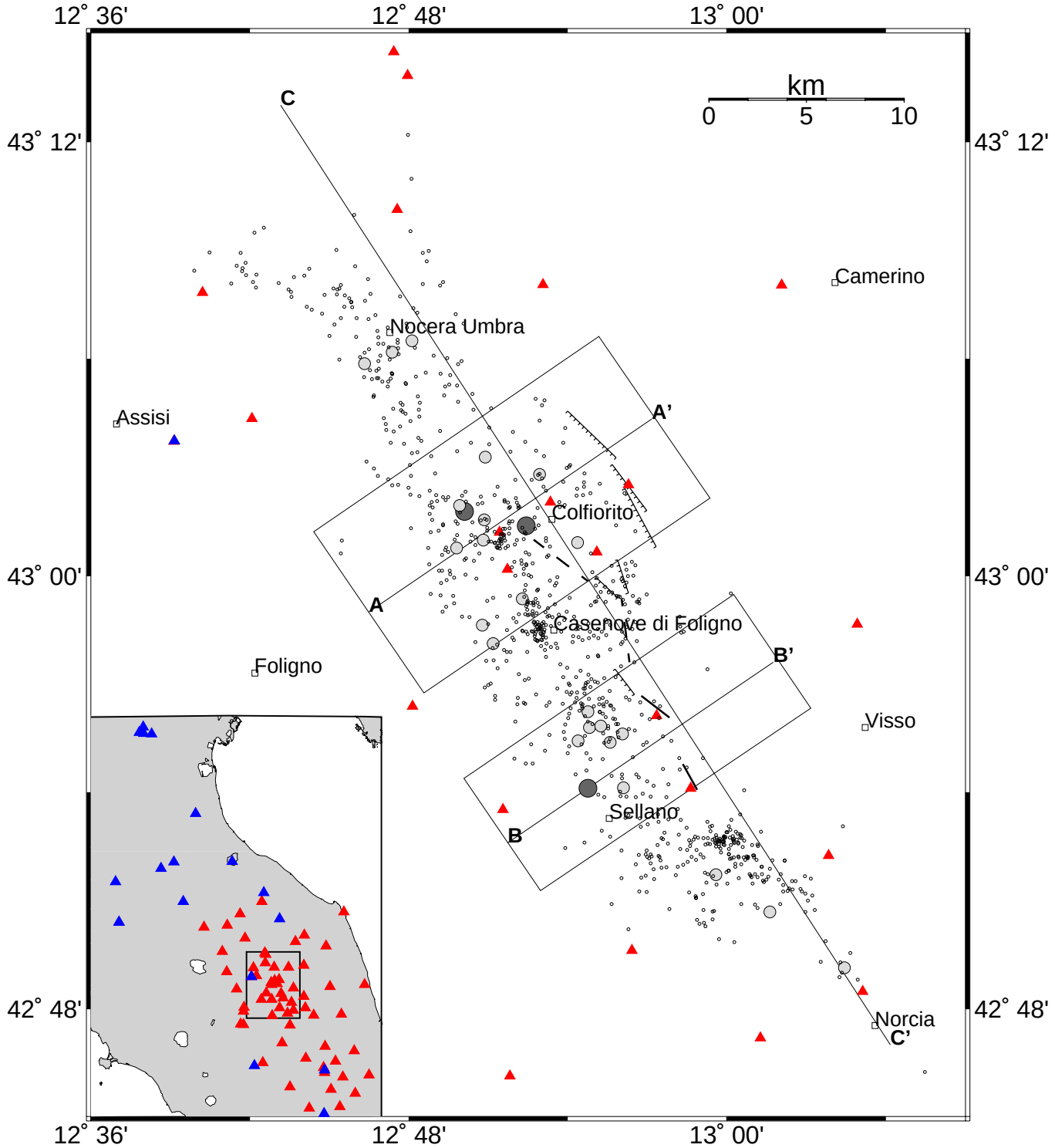
12° 36'
12° 48'
13° 00'
43° 12'
43° 00'
42° 48'
km
0
5
10
C
C'
A
A'
B
B'
Nocera Umbra
Assisi
Colfiorito
Camerino
Foligno
Casenove di Foligno
Visso
Sellano
Norcia

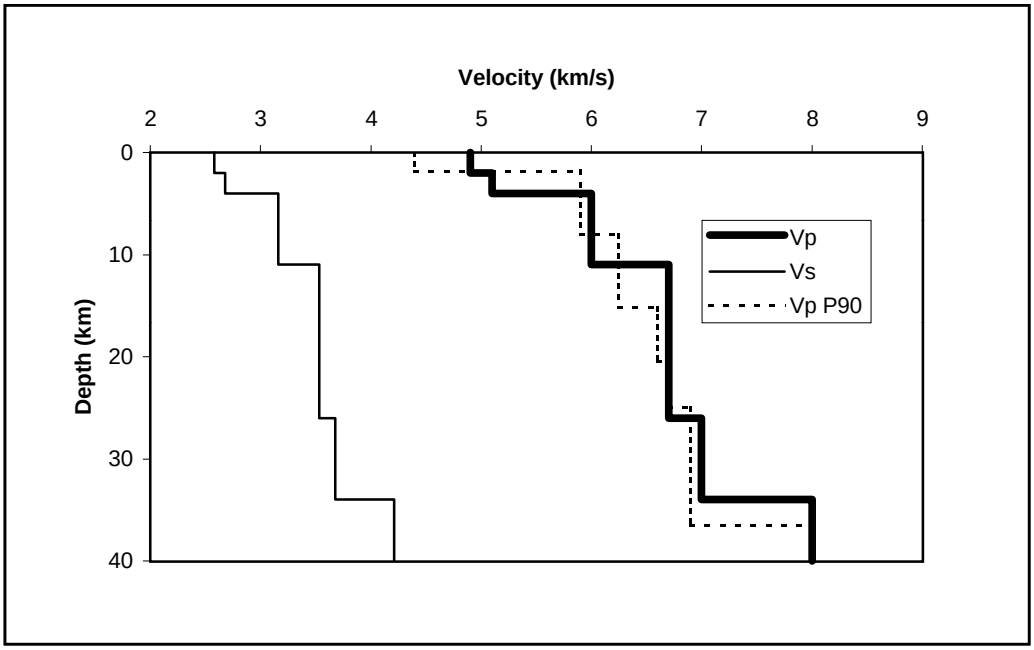

Fig. 5

Fig. 6

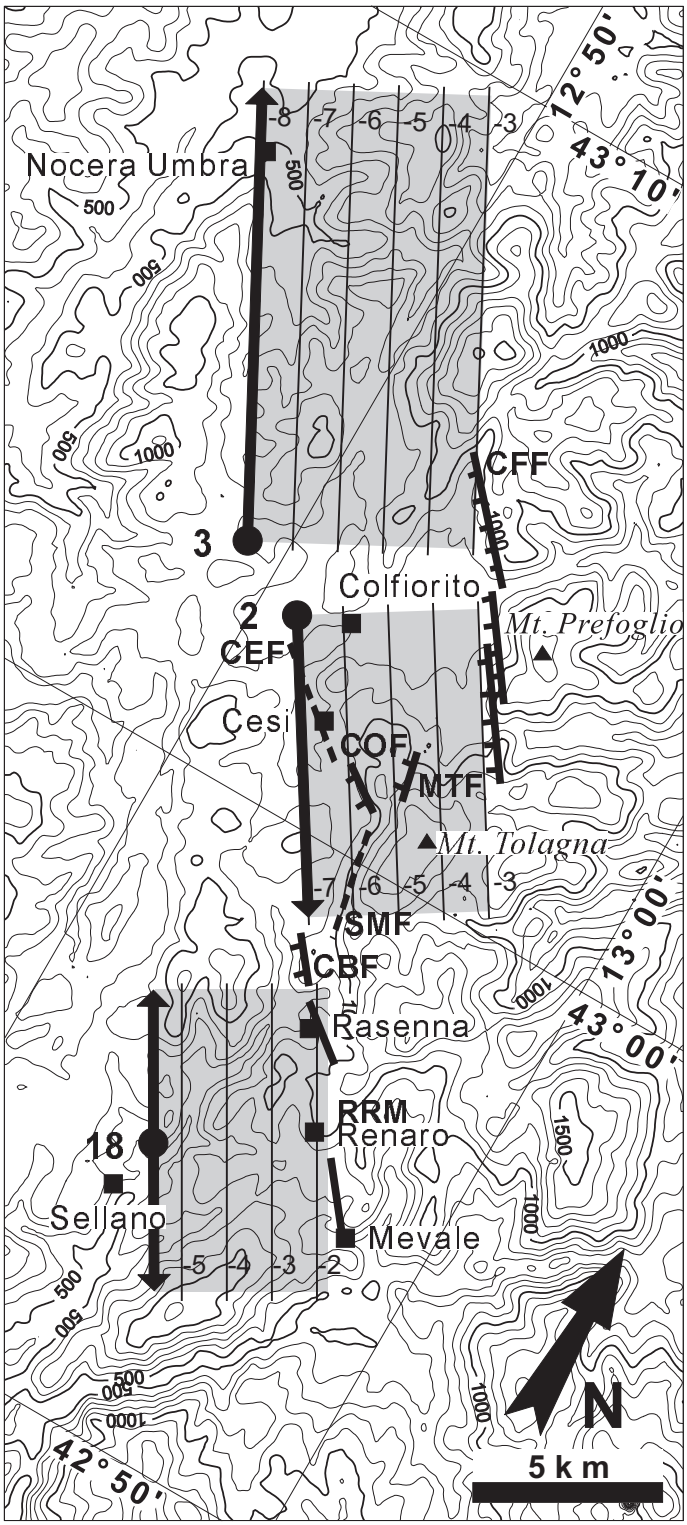
Nocera Umbra
Colfiorito
Mt. Prefoglio
Cesi
Mt. Tolagna
Rasenna
Renaro
Mevale
Sellano
CFF
CEF
COF
MTF
SMF
CBF
RRM
3
2
1
18
-8
-7
-6
-5
-4
-3
-2
500
1000
1500
12° 50'
43° 10'
13° 00'
43° 00'
42° 50'
N
5 k m

Fig. 7

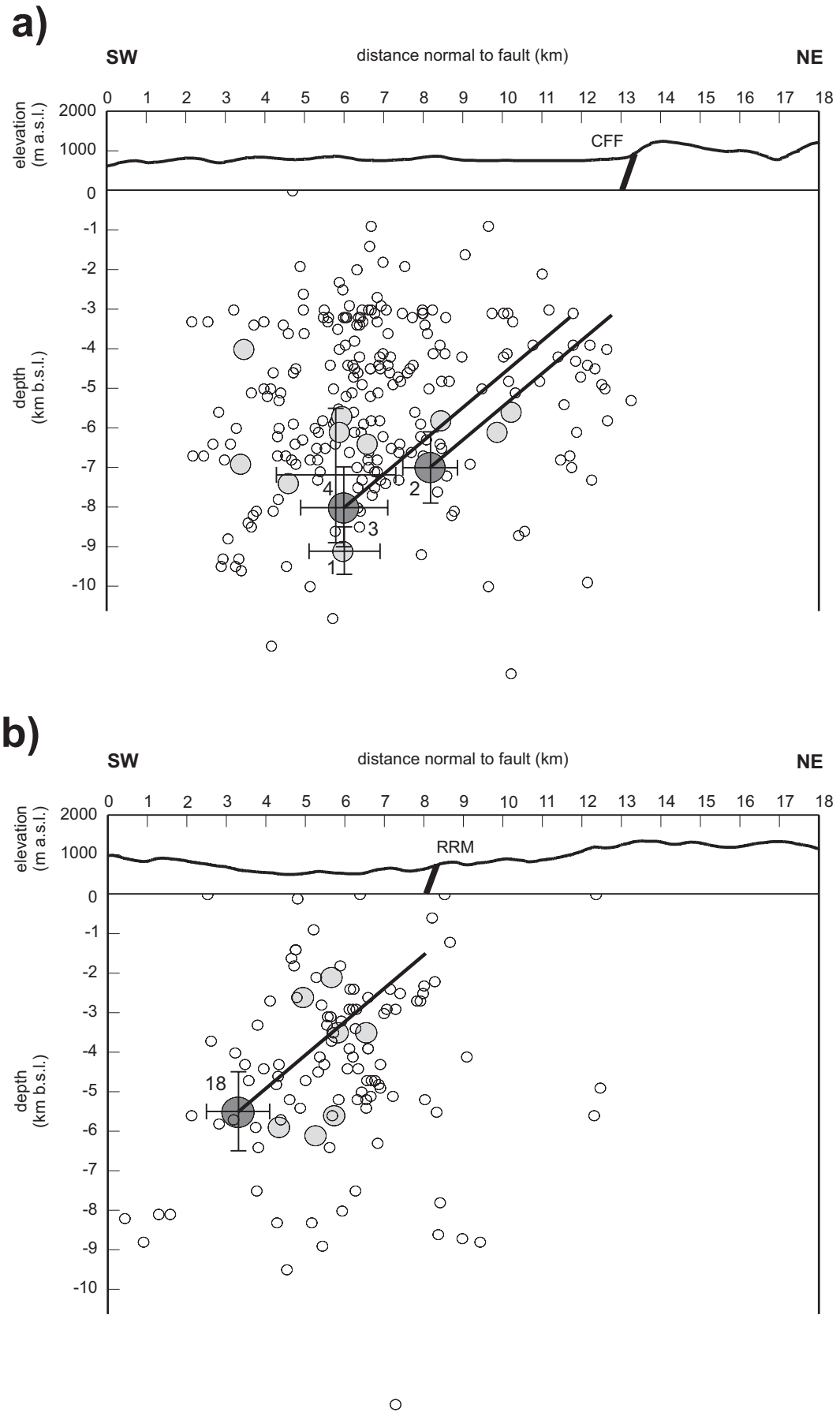
a)
SW
distance normal to fault (km)
NE
elevation (m a.s.l.)
depth (km b.s.l.)
CFF
1
2
3
4
b)
SW
distance normal to fault (km)
NE
elevation (m a.s.l.)
depth (km b.s.l.)
RRM
18

Fig. 8

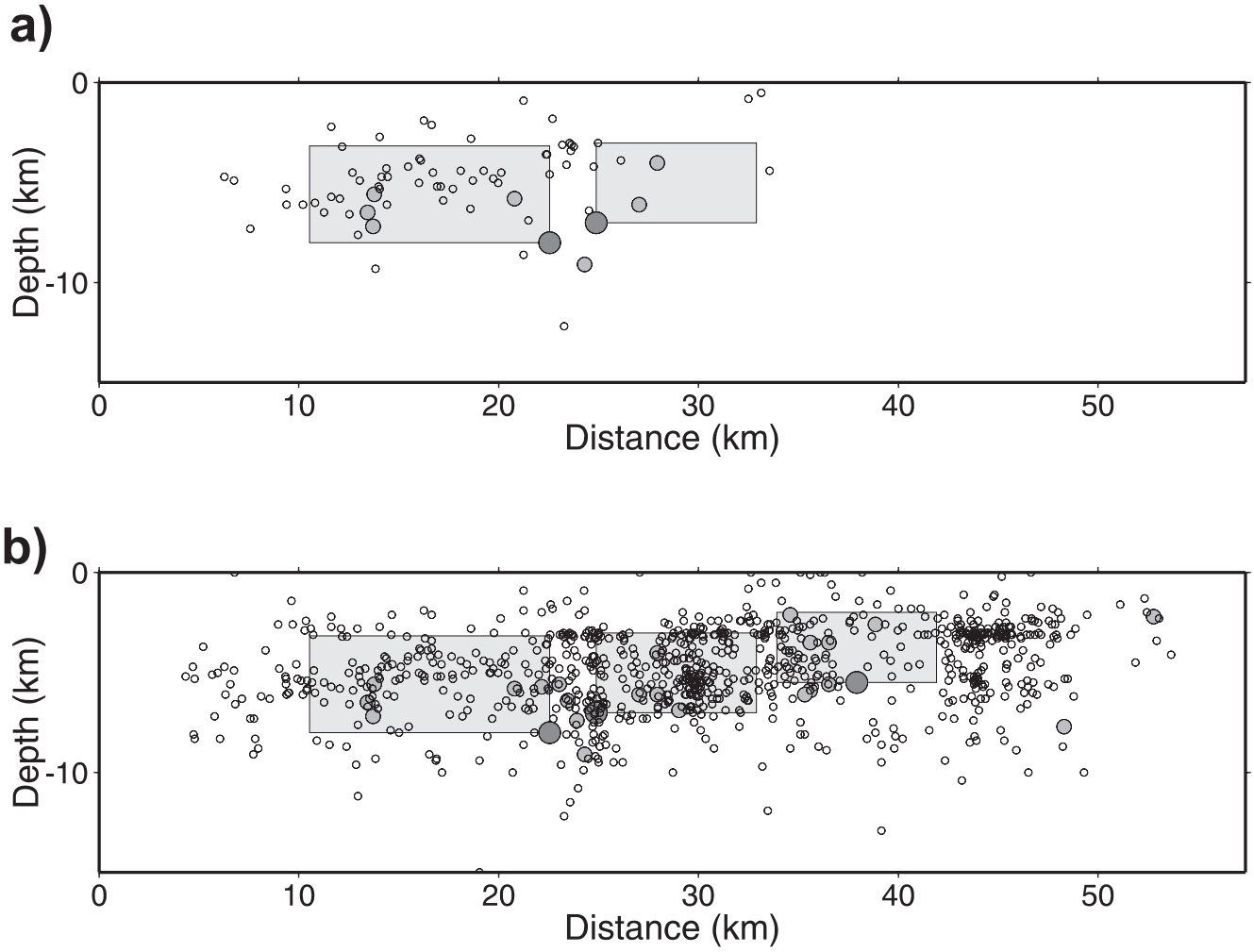
a)
0
-10
Depth (km)
0
10
20
30
40
50
Distance (km)
b)
0
-10
Depth (km)
0
10
20
30
40
50
Distance (km)

Fig. 9

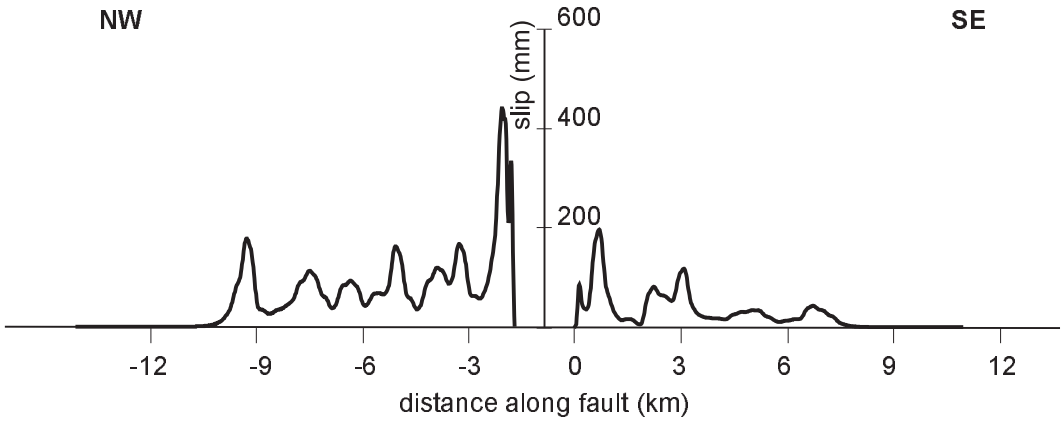
NW
SE
600
400
200
slip (mm)
-12
-9
-6
-3
0
3
6
9
12
distance along fault (km)

Fig. 10

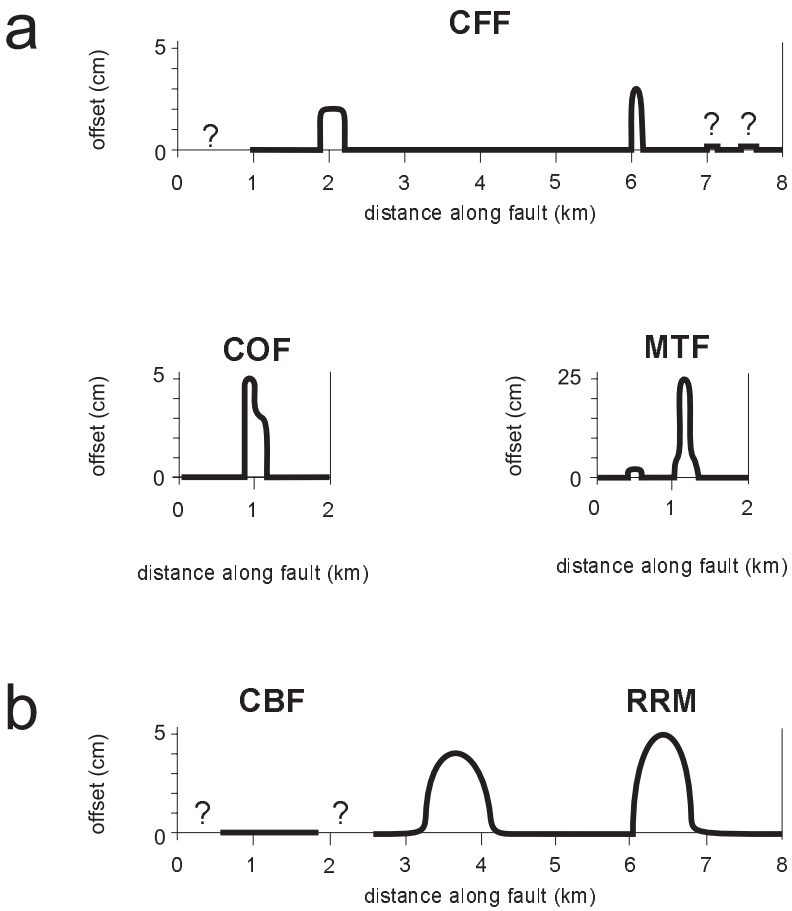
a
CFF
offset (cm)
5
0
?
? ?
0 1 2 3 4 5 6 7 8
distance along fault (km)
COF
offset (cm)
5
0
0 1 2
distance along fault (km)
MTF
offset (cm)
25
0
0 1 2
distance along fault (km)
b
CBF
RRM
offset (cm)
5
0
? ?
0 1 2 3 4 5 6 7 8
distance along fault (km)